Discrimination of A/T Sequences in the Minor Groove of DNA within a Cyclic Polyamide Motif

Christian Melander, David M. Herman, and Peter B. Dervan*[a]

Abstract: Eight-ring cyclic polyamides containing pyrrole (Py), imidazole (Im), and hydroxypyrrole (Hp) aromatic amino acids recognize predetermined six base pair sites in the minor groove of DNA. Two four-ring polyamide subunits linked by (*R*)-2,4-diaminobutyric acid [$(R)^{H_2N}\gamma$] residue form hairpin polyamide structures with enhanced DNA binding properties. In hairpin polyamides, substitution of Hp/Py for Py/Py pairs enhances selectivity for T·A base pairs but compromises binding affinity for specific sequences. In an effort to enhance the binding properties of polyamides containing Hp/Py pairings, four eight ring cyclic polyamides were synthesized and analyzed on a DNA restriction fragment containing three 6-bp sites 5′-tAGNNCTt-3′, where NN = AA, TA, or AT. Quantitative footprint titration experiments demonstrate that contiguous placement of Hp/Py pairs in cyclo-(γ-ImPyPyPy-$(R)^{H_2N}\gamma$-ImHpHpPy-) (**1**) provides a 20-fold increase in affinity for the 5′-tAGAACTt-3′ site ($K_a = 7.5 \times 10^7\,M^{-1}$) relative to ImPyPyPy-$(R)^{H_2N}\gamma$-ImHpHpPy-C3-OH (**2**). A cyclic polyamide of sequence composition cyclo-(γ-ImHpPyPy-$(R)^{H_2N}\gamma$-ImHpPyPy-) (**3**) binds a 5′-tAGTACTt-3′ site with an equilibrium association constant $K_a = 3.2 \times 10^9\,M^{-1}$, representing a fivefold increase relative to the hairpin analogue ImHpPyPy-$(R)^{H_2N}\gamma$-ImHpPyPy-C3-OH (**4**). Arrangement of Hp/Py pairs in a 3′-stagger regulates specificity of cyclo-(γ-ImPyHpPy-$(R)^{H_2N}\gamma$-ImPyHpPy-) (**5**) for the 5′-tAGATCTt-3′ site ($K_a = 7.5 \times 10^7\,M^{-1}$), threefold increase in affinity relative to the hairpin analogue ImPyHpPy-$(R)^{H_2N}\gamma$-ImPyHpPy-C3-OH (**6**), respectively. This study identifies cyclic polyamides as a viable motif for restoring recognition properties of polyamides containing Hp/Py pairs.

Keywords: A·T-specificity · base pairing · cyclic Hp polyamides · DNA recognition · hydrogen bonds

Introduction

Polyamides containing the three aromatic amino acids pyrrole (Py), imidazole (Im), and 3-hydroxypyrrole (Hp), are cell permeable synthetic ligands[1] which recognize predetermined sequences of DNA at subnanomolar concentrations and may be useful for gene regulation studies.[2] DNA recognition depends on a of side-by-side aromatic amino acid pairings that are oriented N–C with respect to the 5′ → 3′ direction of the DNA helix in the minor groove. An antiparallel pairing of Im opposite Py (Im/Py pair) distinguishes G·C from C·G, pairing of Py opposite Im (Py/Im) distinguishes C·G from G·C and both of these from A·T/T·A base pairs.[2] A Py/Py pair binds both A·T and T·A in preference to G·C/C·G.[2] A Hp/Py pair specifies T·A from A·T, while Py/Hp targets A·T in preference to T·A and both of these from G·C/C·G, completing recognition of the four Watson–Crick base pairs.[3]

In parallel with elucidation of the scope and limitations of the polyamide pairing rules, efforts have been made to increase DNA binding affinity and sequence specificity by covalently linking polyamide subunits. A hairpin polyamide motif with γ-aminobutyric acid (γ) serving as a turn-specific internal-guide-residue provides specific binding to designated target sites with >100-fold enhanced affinity relative to the unlinked subunits.[2] Hairpins have the important feature that ring pairings are set in place unambiguously as compared to homodimers which can afford "slipped motifs".[4] Replacement of the γ-turn residue with the chiral subunit (*R*)-2,4-diaminobutyric acid ($(R)^{H_2N}\gamma$) enhances hairpin DNA-binding affinity, sequence specificity, and orientational preference.[2] Further modification of hairpin polyamides by covalently tethering the N- and C-termini with a second γ-turn provides a cyclic polyamide motif that recognizes target sequences with increased affinity and specificity.[2]

Hp/Py hairpin polyamides: High resolution X-ray diffraction data reveals that the T·A selectivity of the Hp/Py pair arises from a combination of i) shape selection of an asymmetric cleft of the floor of the minor groove by the O2 of thymine and C2–H of adenine and ii) specific hydrogen bonds between the 3-hydroxy and 4-carboximido groups of Hp with the O2 of T (Figure 1).[3b] The gain in specificity, however, is accompanied by an energetic penalty. Replacement of a single Py/Py pair

[a] Prof. P. B. Dervan, C. Melander, D. M. Herman
Arnold and Mabel Beckman Laboratories of Chemical Synthesis
California Institute of Technology, Pasadena, CA 91125 (USA)
Fax: (+1) 626-568-8824
E-mail: dervan@cco.caltech.edu

  0947-6539/00/0624-4487 $ 17.50+.50/0

with a Hp/Py pair results in a fivefold destabilization of an eight ring hairpin for an identical match site.[3a–c] Surprisingly, addition of multiple Hp/Py pairs for Py/Py pairs in a 10-ring hairpin polyamide results in a modest tenfold reduction in affinity for the same site; this illustrates that loss in binding affinity is not always additive as the number of Hp/Py substitutions is increased.[3d] Crystallographic data reveals that Hp/Py polyamides bind undistorted B-form DNA, however, a localized 0.5 Å melting of the T·A Watson–Crick base pair is observed when the ImHpPyPy-Dp dimer is bound to 5′-AGTACT-3′ and is potentially responsible for the energetic destabilization of the Hp/Py pair relative to the Py/Py pair.[3b] A subsequent crystallographic study of an $(ImPyHpPy\text{-}Dp)_2$·5′-AGATCT-3′ complex did not reveal such a melting and it is uncertain at this time the extent base pair melting contributes to binding destabilization.[3e] In either case, reduction of affinity is observed and thus provides impetus to elucidate structural elements that restore polyamide binding properties to those comparable to naturally occurring DNA binding proteins without loss of specificity.

Cycle motif: As a test case we consider discrimination of the three six base pair sequence 5′-WGNNCW-3′, where NN = AA, TA, and AT, which are bound by parent compounds ImPyPyPy-$(R)^{H_2N}\gamma$-ImPyPyPy-C3-OH (**1**) and cyclo-(γ-ImPyPyPy-$(R)^{H_2N}\gamma$-ImPyPyPy-) (**2**) containing central Py/Py pairs with *high affinity* but *modest discrimination* of the core AA, TA, and AT sequences as expected by Py/Py degenerate recognition of A·T/T·A base pairs. Replacement of the two central Py/Py pairs with Hp/Py pairs in varying spatial arrangements within the hairpin and cycle motifs allows us to compare the magnitude of the energetic penalty versus the gain or loss in sequence specificity for each motif. To determine if cyclization is a viable strategy for restoring the DNA binding properties of multiple Hp/Py pairings, three eight ring hydroxypyrrole hairpins and their cyclic analogues were synthesized by solid-phase methods;[5] ImPyPyPy-$(R)^{H_2N}\gamma$-ImHpHpPy-C3-OH (**3**), cyclo-(γ-ImPyPyPy-$(R)^{H_2N}\gamma$-ImHpHpPy-) (**4**), ImHpPyPy-$(R)^{H_2N}\gamma$-ImHpPyPy-C3-OH (**5**), cyclo-(γ-ImHpPyPy-$(R)^{H_2N}\gamma$-ImHpPyPy-) (**6**), ImPyHpPy-$(R)^{H_2N}\gamma$-ImPyHpPy-C3-OH (**7**), and cyclo-(γ-ImPyHpPy-$(R)^{H_2N}\gamma$-ImPyHpPy-) (**8**) (Figure 2). Equilibrium association constants (K_a) for the eight polyamides were determined by quantitative DNase I footprint titration[6] experiments on a DNA fragment containing three six base pair binding sites 5′-AGAACT-3′, 5′-AGTACT-3, and 5′-

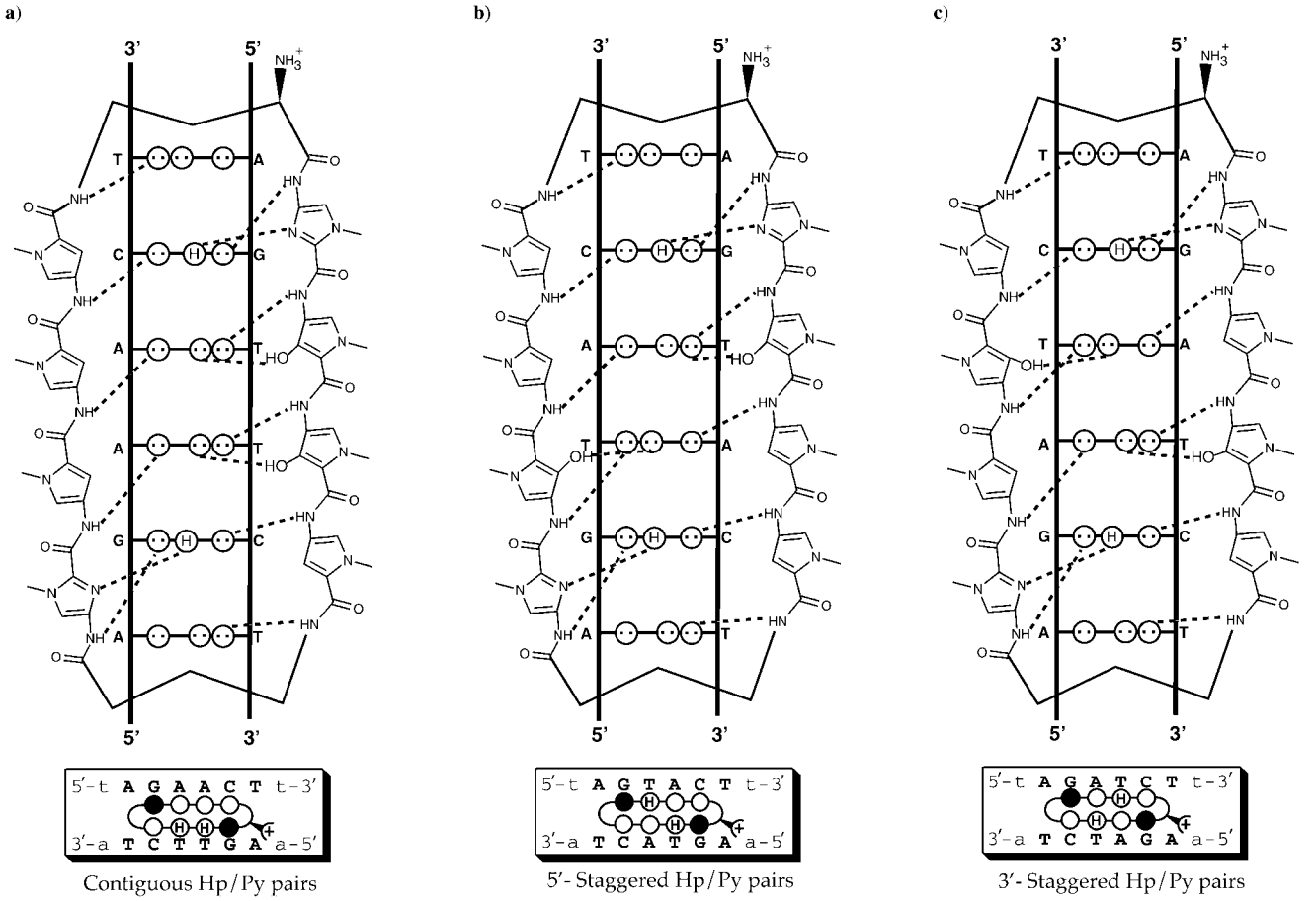

Figure 1. Top: Hydrogen bond models of the 1:1 polyamide–DNA complexes formed between cyclo-(γ-ImPyPyPy-$(R)^{H_2N}\gamma$-ImHpHpPy-) (**4**), cyclo-(γ-ImHpPyPy-$(R)^{H_2N}\gamma$-ImHpPyPy-) (**6**), and cyclo-(γ-ImPyHpPy-$(R)^{H_2N}\gamma$-ImPyHpPy-) (**8**), and their respective six base pair match sites 5′-tAGAACTt-3′, 5′-tAGTACTt-3′, and 5′-tAGATCTt-3′. Circles with dots represent lone pairs of N3 of purines and O2 of pyrimidines. Circles containing an H, Ⓗ, represent the N2 hydrogen of guanine. Putative hydrogen bonds are illustrated by dotted lines. Bottom: For schematic binding model, Im and Py rings are represented as shaded and unshaded spheres respectively, while Hp rings are annotated with an "H" in the center of an unshaded sphere. Flanking sequences are designated in lower case, regular type while the respective binding sites are given in capital bold type.

0947-6539/00/0624-4488 $ 17.50+.50/0 *Chem. Eur. J.* **2000**, *6*, No. 24

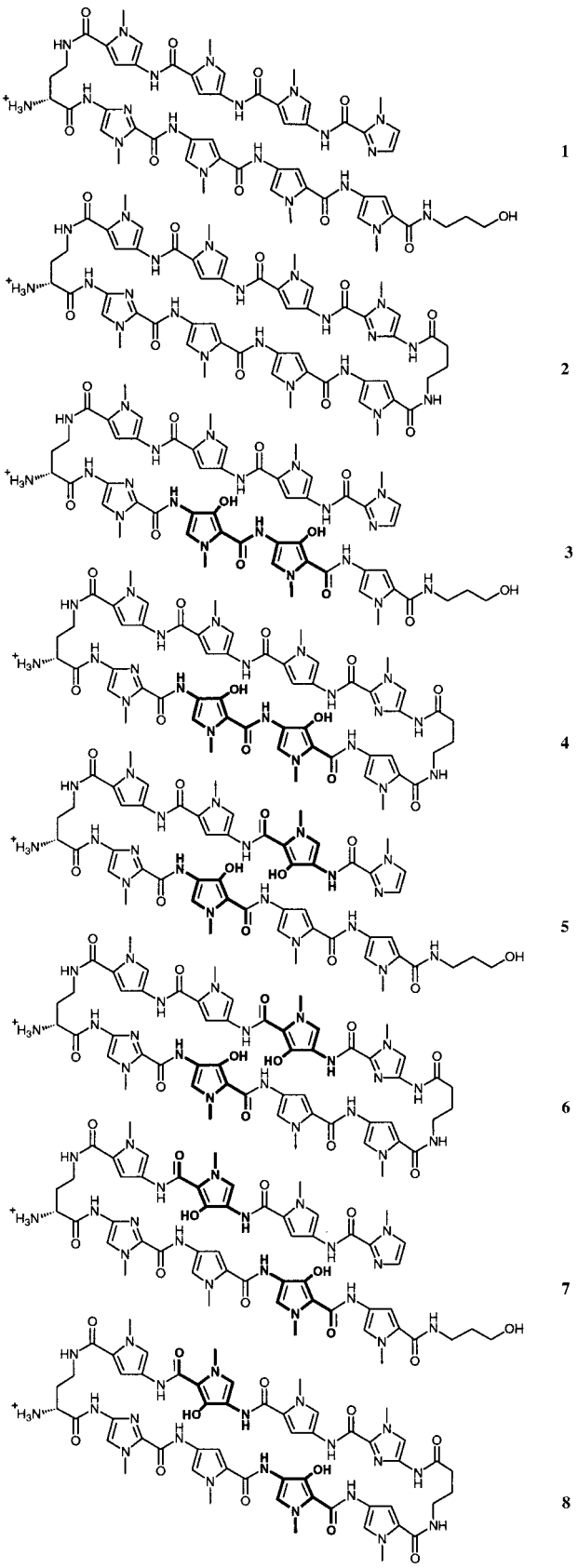

Figure 2. Structures of the eight ring polyamides ImPyPyPy-$(R)^{H_2N}\gamma$-ImPyPyPy-C3-OH (**1**), cyclo-(γ-ImPyPyPy-$(R)^{H_2N}\gamma$-ImPyPyPy-) (**2**), ImPyPyPy-$(R)^{H_2N}\gamma$-ImHpHpPy-C3-OH (**3**), cyclo-(γ-ImPyPyPy-$(R)^{H_2N}\gamma$-ImHpHpPy-) (**4**), ImHpPyPy-$(R)^{H_2N}\gamma$-ImHpPyPy-C3-OH (**5**), cyclo-(γ-ImHpPyPy-$(R)^{H_2N}\gamma$-ImHpPyPy-) (**6**), ImPyHpPy-$(R)^{H_2N}\gamma$-ImPyHpPy-C3-OH (**7**), and cyclo-(γ-ImPyHpPy-$(R)^{H_2N}\gamma$-ImPyHpPy-) (**8**).

AGATCT-3′. Based on the pairing rules, polyamides **3** and **4** with contiguous Hp residues bind 5′-AGAACT-3′ as a match site and 5′-AGATCT-3′ and 5′-AGTACT-3′ as single base pair mismatch sites. Polyamides **5** and **6** which provide Hp residues staggered towards the 5′-direction relative to the DNA helix, target 5′-AGTACT-3′ as a match, 5′-AGAACT-3′ as a single base pair mismatch, and 5′-AGATCT-3′ as a double base pair mismatch. Compounds **7** and **8**, containing a 3′-stagger of Hp residues, preferentially target 5′-AGATCT-3′, relative to the single and double base pair mismatch sites, 5′-AGAACT-3′ and 5′-AGTACT-3′, respectively. It might have been anticipated that the flexible hairpin can slide for optimal ligand–minor groove contacts, and that the constraints of preorganized cycles would not be beneficial for the Hp/Py pair: T·A recognition. Remarkably our findings are just the opposite and form the basis for our report here.

Results and Discussion

Hairpin polyamide syntheses: Polyamide **1** was prepared as previously described.[7a] Three polyamide resins, ImPyPyPy-$(R)^{Fmoc}\gamma$-ImOpOpPy-β-PAM resin, ImOpPyPy-$(R)^{Fmoc}\gamma$-ImOpPy-β-PAM resin, and ImPyOpPy-$(R)^{Fmoc}\gamma$-ImPyOpPy-β-PAM resin were synthesized from commercially available Boc-β-alanine-PAM resin (0.5 g resin, 0.25 mmol g^{-1} substitution) using manual, solid-phase protocols in 18 steps (Figure 3).[5] The Fmoc protecting group was then removed by treatment with piperidine/DMF 4:1 (22 °C, 30 min) to provide ImPyPyPy-$(R)^{H_2N}\gamma$-ImOpOpPy-β-PAM, ImOpPyPy-$(R)^{H_2N}\gamma$-ImOpPyPy-β-PAM, and ImPyOpPy-$(R)^{H_2N}\gamma$-ImPyOpPy-β-PAM resins. The polyamide was then cleaved from resin by a single-step reductive cleavage reaction with $NaBH_4$/THF (60 °C, 5 h).[8] The reaction mixture was subsequently purified by reversed-phase HPLC to provide the methoxy-protected analogues ImPyPyPy-$(R)^{H_2N}\gamma$-ImOpOpPy-C3-OH (**9**), ImOpPyPy-$(R)^{H_2N}\gamma$-ImOpPyPy-C3-OH (**10**), and ImPyOpPy-$(R)^{H_2N}\gamma$-ImPyOpPy-C3-OH (**11**). Deprotection with sodium thiophenoxide/DMF (100 °C, 2 h)[3e] and purification by reversed-phase HPLC yielded polyamides ImPyPyPy-$(R)^{H_2N}\gamma$-ImHpHpPy-C3-OH (**3**), ImHpPyPy-$(R)^{H_2N}\gamma$-ImHpPyPy-C3-OH (**5**), and ImPyHpPy-$(R)^{H_2N}\gamma$-ImPyHpPy-C3-OH (**7**).

Cyclic polyamide syntheses: Polyamide **2** was synthesized as previously described.[7a] Three polyamide resins, Bocγ-ImPyPyPy-$(R)^{Fmoc}\gamma$-ImOpOpPy-PAM resin, Bocγ-ImOpPyPy-$(R)^{Fmoc}\gamma$-ImOpPyPy-PAM resin, and Bocγ-ImPyOpPy-$(R)^{Fmoc}\gamma$-ImPyOpPy-PAM resin, were synthesized in 18 steps from Boc-Py-PAM resin (1.0 g resin, 0.5 mmol g^{-1} substitution) using Boc-chemistry and manual solid-phase synthesis protocols (Figure 4).[5, 7a] The (*R*)-2,4-diaminobutyric acid residue was introduced as an orthogonally protected *N*-α-Fmoc-*N*-γ-Boc derivative (HBTU, DIEA). Boc protected resins Bocγ-ImPyPyPy-$(R)^{Fmoc}\gamma$-ImOpOpPy-PAM resin, Bocγ-ImOpPyPy-$(R)^{Fmoc}\gamma$-ImOpPyPy-PAM resin, and Bocγ-ImPyOpPy-$(R)^{Fmoc}\gamma$-ImPyOpPy-PAM resin, were treated with TFA/CH_2Cl_2/thiophenol 80%: 20%: 0.4 M (22 °C, 30 min) to provide $H_2N\gamma$-ImPyPyPy-$(R)^{Fmoc}\gamma$-ImOpOpPy-PAM resin, $H_2N\gamma$-ImOpPyPy-$(R)^{Fmoc}\gamma$-ImOpPyPy-PAM resin, and $H_2N\gamma$-ImPyOpPy-$(R)^{Fmoc}\gamma$-ImPyOpPy-PAM resin.

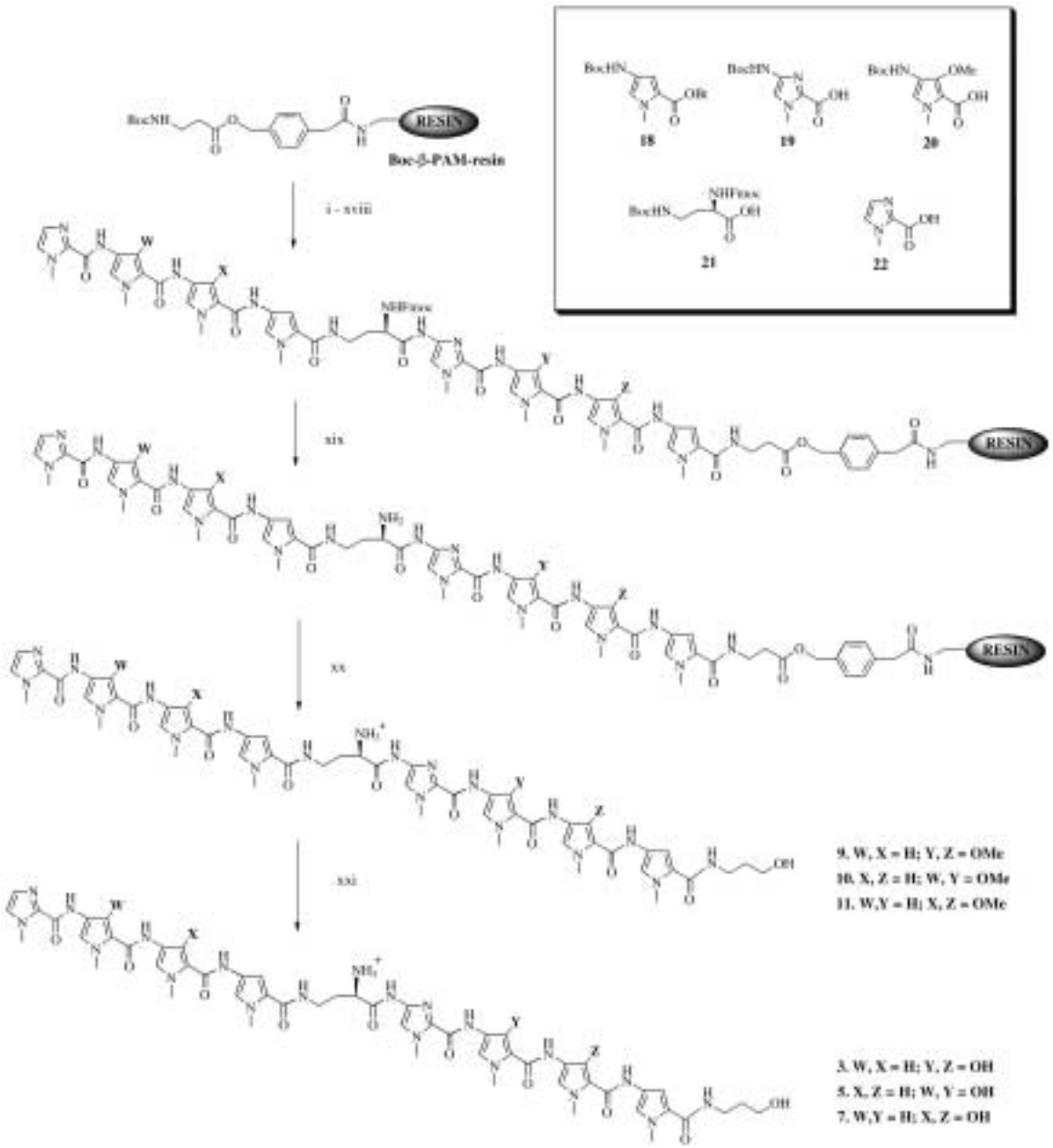

Figure 3. Hairpin synthetic scheme. ImPyPyPy-$(R)^{H_2N}\gamma$-ImHpHpPy-C3-OH (**3**): i) 80% TFA/DCM, 0.4 M PhSH; ii) Boc-Py-OBt, DIEA, DMF; iii) 80% TFA/DCM, 0.4 M PhSH; iv) Boc-Op-OH, HBTU, DIEA, DMF; v) 80% TFA/DCM, 0.4 M PhSH; vi) Boc-Op-OH, HBTU, DIEA, DMF; vii) 80% TFA/DCM, 0.4 M PhSH; viii) Boc-Im-OH, DIEA, HBTU, DMF; ix) 80% TFA/DCM, 0.4 M PhSH; x) Fmoc-α-Boc-γ-diaminobutyric acid HBTU, DIEA); xi) 80% TFA/DCM, 0.4 M PhSH; xii) Boc-Py-OBt, DIEA, DMF; xiii) 80% TFA/DCM, 0.4 M PhSH; xiv) Boc-Py-OBt, DIEA, DMF; xv) 80% TFA/DCM, 0.4 M PhSH; xvi) Boc-Py-OBt, DIEA, DMF; xvii) 80% TFA/DCM, 0.4 M PhSH; xviii) imidazole-2-carboxylic acid (HBTU/DIEA); xix) 80% piperidine/DMF (25 °C, 30 min) xx) $NaBH_4$/THF; xxi) sodium thiophenoxide/DMF. ImHpPyPy-$(R)^{H_2N}\gamma$ImHpPyPy-C3-OH (**5**): i) – iii), v) – xiii), xv) – xxi) same as above; iv) Boc-Py-OH, HBTU, DIEA, DMF; xiv) Boc-Op-OH, HBTU, DIEA, DMF. ImPyHpPy-$(R)^{H_2N}\gamma$ImPyHpPy-C3-OH (**7**): i) – v), vii) – xiii), xiv) – xxi) same as above; vi) Boc-Py-OBt, DIEA, DMF; xiv) Boc-Op-OH, HBTU, DIEA, DMF. (Inset) Py, Im, Op, and diaminobutyric acid monomers for solid-phase synthesis: Boc-pyrrole-OBt ester[5] (Boc-Py-OBt) **18**, Boc-imidazole-OH **19**, Boc-Op-OH **20**, (*R*)-Fmoc-γ-Boc-γ-diaminobutyric acid **21**, imidazole-2-carboxylic acid[14] (Im-OH) **22**.

Following protection as the benzyl carbamate using Cbz-OSu (DMF, 22 °C, 90 min), Cbzγ-ImPyPyPy-$(R)^{Fmoc}\gamma$-ImOpOpPy-PAM resin, Cbzγ-ImOpPyPy-$(R)^{Fmoc}\gamma$-ImOpPyPy-PAM resin, and Cbzγ-ImPyOpPy-$(R)^{Fmoc}\gamma$-ImPyOpPy-PAM resin, were treated with piperidine/DMF 4:1 (22 °C, 30 min) to provide Cbzγ-ImPyPyPy-$(R)^{H_2N}\gamma$-ImOpOpPy-PAM, Cbzγ-ImOpPyPy-$(R)^{H_2N}\gamma$-ImOpPyPy-PAM, and Cbzγ-ImPyOpPy-$(R)^{H_2N}\gamma$-ImPyOpPy-PAM resins, respectively. The resulting amine resins were then treated with Boc-anhydride (DMF, DIEA, 22 °C, 50 min) producing Cbzγ-ImPyPyPy-$(R)^{Boc}\gamma$-ImOpOpPy-PAM, Cbzγ-ImOpPyPy-$(R)^{Boc}\gamma$-ImOpPyPy-PAM, and Cbzγ-ImPyOpPy-$(R)^{Boc}\gamma$-ImPyOpPy-PAM resins. A sample of each resin was then taken and the respective peptides were liberated from the resin with concomitant removal of the Cbz protecting group by reductive cleavage employing $Pd(OAc)_2$/DMF/water/ammonium formate (37 °C, 14 h).[7a] Following removal of the resin by filtration, the crude reaction mixtures were purified by reversed-phase HPLC to

0947-6539/00/0624-4490 $ 17.50+.50/0 *Chem. Eur. J.* **2000**, *6*, No. 24

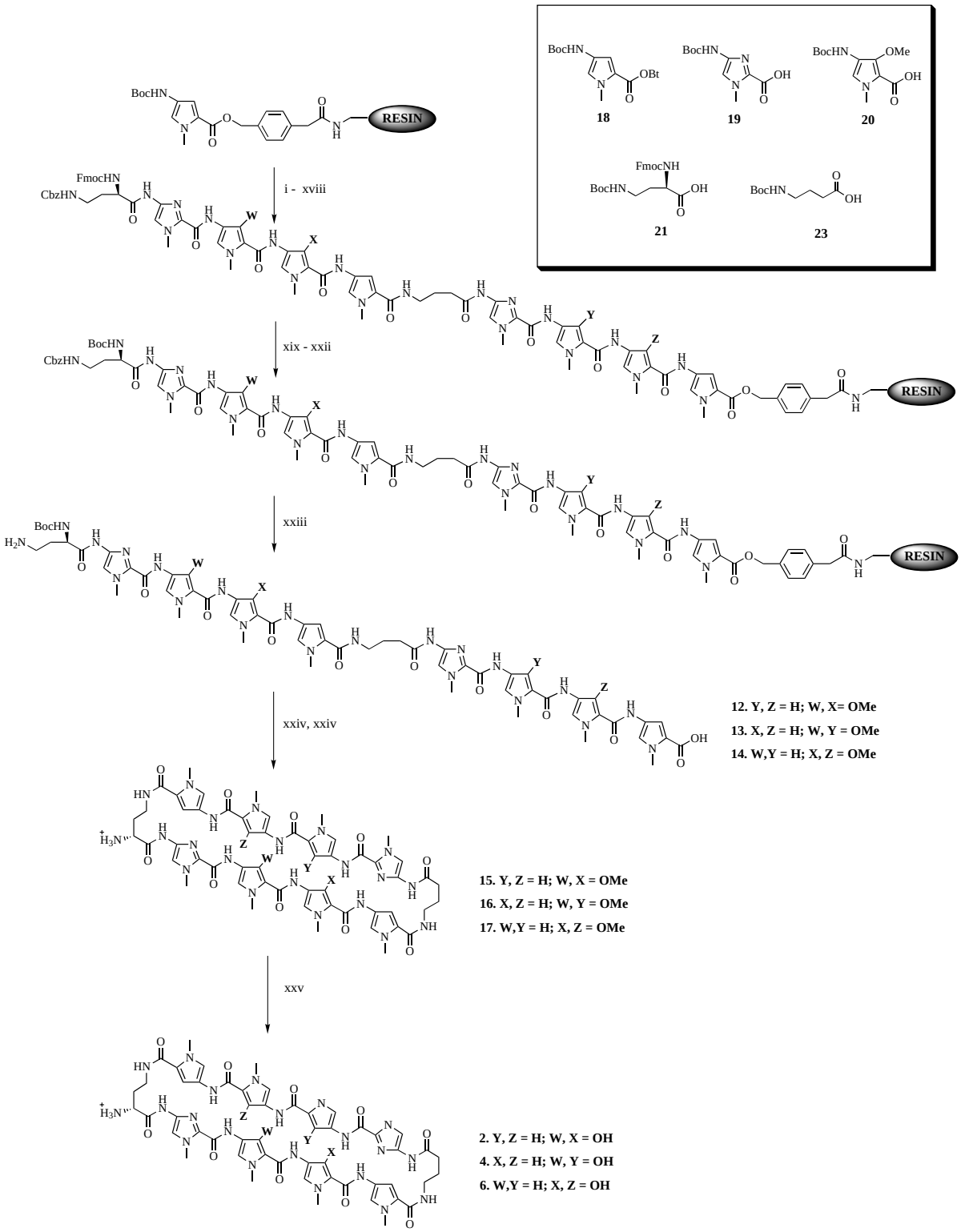

Figure 4. Cycle synthetic scheme. cyclo-(γ-ImPyPyPy-(R)$^{H_2N}\gamma$-ImHpHpPy-) (**4**): i) 80% TFA/DCM, 0.4 M PhSH; ii) Boc-Py-OBt, DIEA, DMF; iii) 80% TFA/DCM, 0.4 M PhSH; iv) Boc-Py-OBt, HBTU, DIEA, DMF; v) 80% TFA/DCM, 0.4 M PhSH; vi) Boc-Im-OH, DIEA, HBTU, DMF; vii) 80% TFA/DCM, 0.4 M PhSH; viii) Boc-γ-diaminobutyric acid (HBTU, DIEA); ix) 80% TFA/DCM, 0.4 M PhSH; x) Boc-Py-OBt, DIEA, DMF; xi) 80% TFA/DCM, 0.4 M PhSH; xii) Boc-Op-OH, HBTU, DIEA, DMF; xiii) 80% TFA/DCM, 0.4 M PhSH; xiv) Boc-Op-OH, HBTU, DIEA, DMF; xv) 80% TFA/DCM, 0.4 M PhSH; xvi) Boc-Im-OH, DIEA, HBTU, DMF; xvii) 80% TFA/DCM, 0.4 M PhSH; xviii) Fmoc-α-Boc-γ-diaminobutyric acid (HBTU, DIEA); xix) 80% TFA/DCM, 0.4 M PhSH; xx) Cbz-OSu, DMF; xxi) 80% piperidine/DMF (25 °C, 30 min); xxii) Boc-anhydride, DMF, DIEA; xxiii) $Pd(OAc)_2$/DMF/ammonium formate/H_2O; xxiv) DPPA/K_2CO_3/DIEA; xxv) TFA; xxvi) sodium thiophenoxide/DMF. cyclo-(γ-ImHpPyPy-(R)$^{H_2N}\gamma$-ImHpPyPy) (**6**): i) – iii), v) – xi), xiii) – xxvi) same as above; iv) Boc-Op-OH, HBTU, DIEA, DMF; xii) Boc-Py-OBt, DIEA, DMF. cyclo-(γ-ImPyHpPy-(R)$^{H_2N}\gamma$-ImPyHpPy-)(**8**): i), iii) – xiii), xv) – xxvi) same as above; vi) Boc-Op-OH, HBTU, DIEA, DMF; xiv) Boc-Py-OBt, DIEA, DMF. (Inset) Py, Im, Op, and diaminobutyric acid monomers for solid-phase synthesis: Boc-Py-OBt[5] **18**, Boc-imidazole-OH **19**, Boc-Op-OH **20**, (R)-Fmoc-α-Boc-γ-diaminobutyric acid **21**, Boc-γ-aminobutyric acid **23**.

  0947-6539/00/0624-4491 $ 17.50+.50/0

yield polyamides H_2N-γ-ImOpOpPy-(*R*)^{Boc}γ-ImPyPyPy-OH (**12**), H_2N-γ-ImOpPyPy-(*R*)^{Boc}γ-ImOpPyPy-OH (**13**), and H_2N-γ-ImPyOpPy-(*R*)^{Boc}γ-ImPyOpPy-OH (**14**). Each polyamide was then cyclized by treatment with DPPA/K_2CO_3/DMF (22 °C, 5 h),[7b] all volatiles subsequently removed, the resulting product deprotected in neat TFA, and the crude product purified by reversed-phase HPLC to yield Op polyamides cyclo-(γ-ImPyPyPy-(*R*)^{H_2N}γ-ImOpOpPy-) (**15**) cyclo-(γ-ImOpPyPy-(*R*)^{H_2N}γ-ImOpPyPy-) (**16**) and cyclo-(γ-ImPyOpPy-(*R*)^{H_2N}γ-ImPyOpPy-) (**17**). Finally, polyamides **15**, **16**, and **17** were O-demethylated with sodium thiophenoxide/DMF (100 °C, 2 h)[3e] and purified by reversed-phase HPLC to yield cyclo-(γ-ImPyPyPy-(*R*)^{H_2N}γ-ImHpHpPy-) (**4**), cyclo-(γ-ImHpPyPy-(*R*)^{H_2N}γ-ImHpPyPy-) (**6**), and cyclo-(γ-ImPyHpPy-(*R*)^{H_2N}γ-ImPyHpPy-)(**8**).

Equilibrium association constants: Quantitative DNase I footprint titrations (Tris·HCl (10 mM), KCl (10 mM), $MgCl_2$ (10 mM), and $CaCl_2$ (5 mM), pH 7.0 and 22 °C)[6] were performed on a ^{32}P end-labeled 285-bp DNA restriction fragment of pDEH10 to determine equilibrium association constants (K_a) for polyamides **1**–**8** on three 6-bp binding sites (Figures 5–7). The match sites for the parent hairpin **1** and cyclo **2** are bound at subnanomolar concentrations in the same order: 5′-tAGTACTt-3′ > 5′-tAGAACTt-3′ > 5′-tAGATCTt-3′ (Table 1). Hairpin **3** and cyclo **4**, containing contiguous Hp/Py pairs, bind the 6-bp sites (Table 1) with two to three orders of magnitude lower affinity and in the order: 5′-tAGAACTt-3′ (match) > 5′-tAGT**A**CTt-3′ (mismatch) > 5′-tAG**A**TCTt-3′ (mismatch), where mismatch base pairs are bold. Hairpin **5** and cyclo **6**, with a 5′-stagger of Hp rings, preferentially bind their match sites with higher affinities relative to polyamides **3** and **4**, and all sites in the following order: 5′-tAGTACTt-3′ (match) > 5′-tAG**A**ACTt-3′ (mismatch) > 5′-tAG**AT**CTt-3′ (double mismatch) (Table 1). Hairpin **7** and cyclo **8**, with a 3′-stagger of Hp rings, binds 5′-tAGATCTt-3′ (match), 5′-tAG**A**ACTt-3′ (mismatch) and 5′-tAG**TA**CTt-3′ (double mismatch) sites (Table 1) with lower overall affinity than the 5′-stagger, but cyclo **8** (not hairpin **7**) establishes preference for the cognate match site 5′-tAGATCTt-3′ by a factor of two.

Table 1. Equilibration association constants [M^{-1}] for polyamides.[a–c]

	Polyamide	5′-tAGAACTt-3′	5′-tAGTACTt-3′	5′-tAGATCTt-3′
1	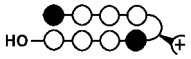	**1.0×10^{10} (0.8)**	**2.1×10^{10} (0.3)**	**4.0×10^{9} (0.3)**
2	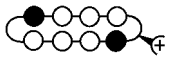	**4.0×10^{10} (0.6)**	**7.0×10^{10} (0.4)**	**5.0×10^{9} (0.3)**
3	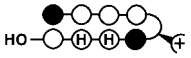	**4.4×10^{6} (0.3)**	1.4×10^{6} (0.5)	$\leq 1 \times 10^{6}$
4	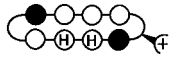	**7.5×10^{7} (1.2)**	1.4×10^{7} (0.3)	$\leq \times 10^{6}$
5	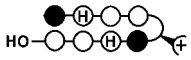	2.6×10^{7} (0.5)	**7.0×10^{8} (1.2)**	$\leq 1 \times 10^{7}$
6	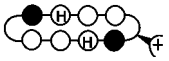	3.5×10^{8} (0.6)	**3.2×10^{9} (1.1)**	$\leq 1 \times 10^{7}$
7	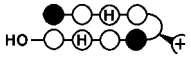	2.0×10^{7} (0.5)	5.4×10^{7} (1.1)	**2.7×10^{7} (0.9)**
8	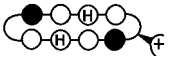	3.5×10^{7} (1.1)	1.4×10^{7} (0.5)	**6.2×10^{7} (1.7)**

[a] Values reported are the mean values obtained from three Dnase I titration experiments. [b] The assays were carried out at 22 °C at pH 7 in the presence of Tris-HCl (10 mm), KCl (10 mm), $MgCl_2$ (10 mm), and $CaCl_2$ (5 mm). [c] Match site equilibrium association constants are shown in bold type.

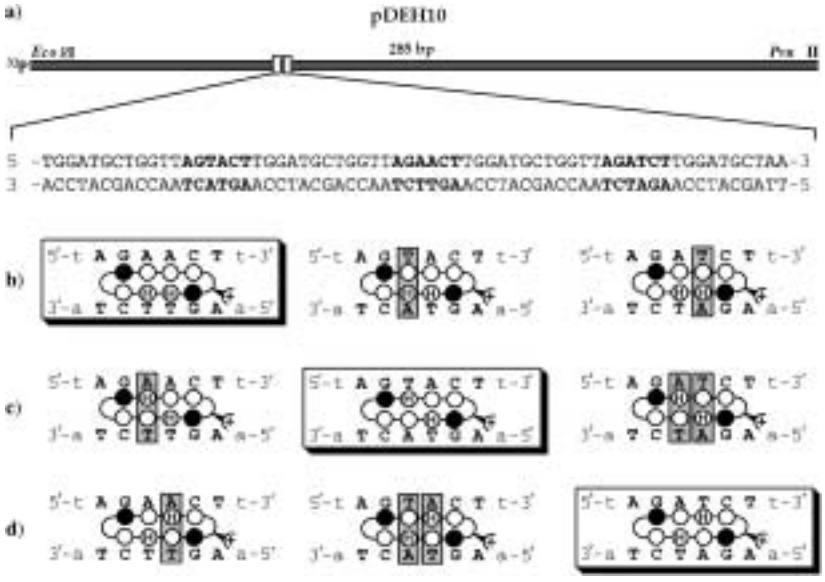

Figure 5. Partial sequence of the synthesized insert from the pDEH10 match and mismatch target sites. a) Illustration of the *Eco*RI/*Pvu*II restriction fragment containing the *Bam*HI and *Hin*dIII insert. The sequences in bold were the only sites analyzed by quantitative DNase I footprint titrations. b)–d) Schematic binding models of cyclo-(γ-ImPyPyPy-(*R*)^{H_2N}γ-ImHpHpPy-) (**4**) cyclo-(γ-ImHpPyPy-(*R*)^{H_2N}γ-ImHpPyPy-) (**6**), and cyclo-(γ-ImPyHpPy-(*R*)^{H_2N}γ-ImPyHpPy-) (**8**) with their putative match and mismatch sites. Im and Py rings are represented as shaded and unshaded spheres, respectively, while Hp rings are annotated with an "H" in the center of an unshaded sphere. Match sites are boxed, and mismatch base pairs are marked with a shaded rectangle.

Specificity of Hp/Py cycles: Comparison of the binding affinities reveals the effects introduction of multiple Hp/Py pairs has on sequence specificity (Table 2). On the basis of the pairing rules for polyamide recognition of DNA complexes, the 5′-tAGAACTt-3′, 5′-tAGTACTt-3′, and 5′-tAGATCTt-3′ are "match" sites for polyamides **1** and **2**. For polyamides **3**–**8**, one of the three binding sites represents a match while the other two sites are single or double base pair mismatches with regard to the Hp/Py pairings. Among the three "match" binding sites for hairpin **1**, 5′-tAGTACTt-3′ was bound with two- to fivefold specificity over the other two sites. Preference

0947-6539/00/0624-4492 $ 17.50+.50/0 *Chem. Eur. J.* **2000**, *6*, No. 24

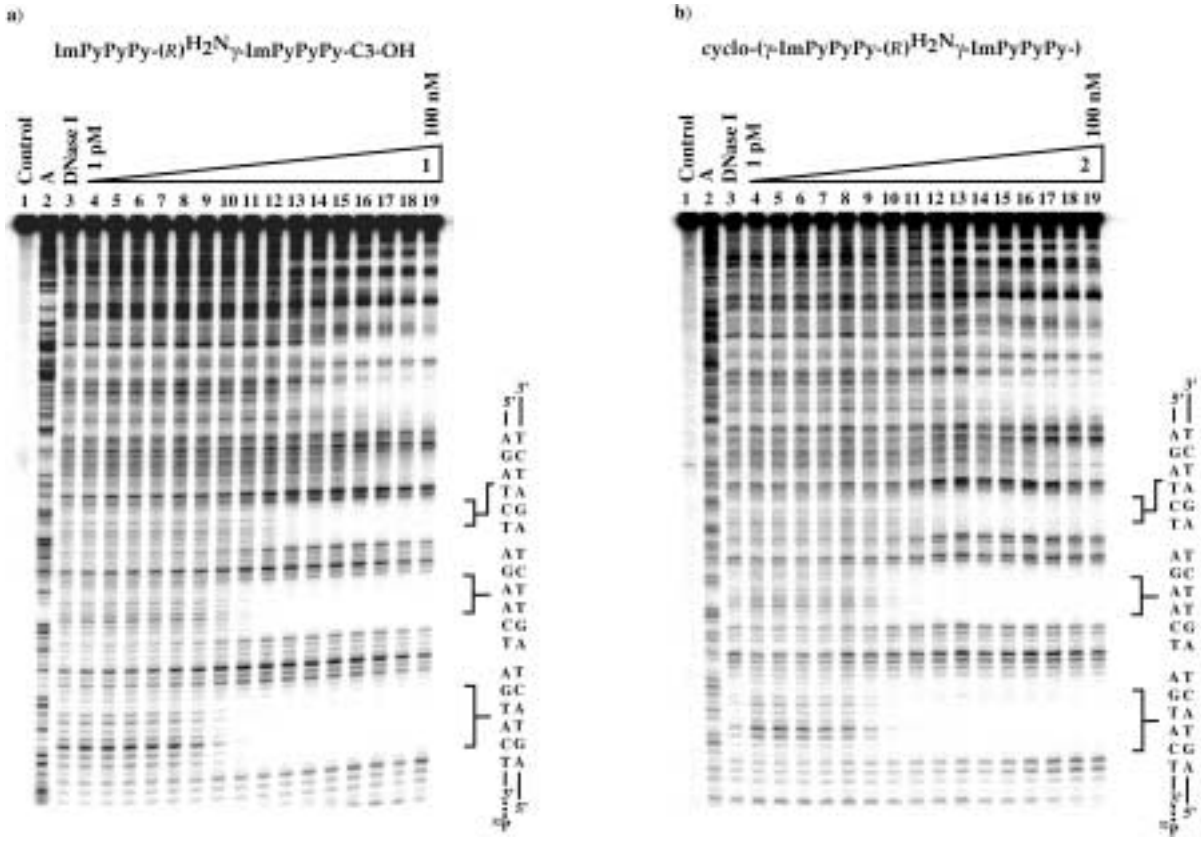

Figure 6. Footprinting experiments on the 3′-^{32}P-labeled 285-bp DNA restriction fragment derived from the plasmid pDEH10. Quantitative DNase I footprint titration experiment with a) ImPyPyPy-(*R*)$^{H_2N}\gamma$-ImPyPyPyPy-C3-OH (**1**): lane 1: intact; lane 2: A reaction; lane 3: DNase I standard; lanes 4–19: 1 pM, 2 pM, 5 pM, 10 pM, 20 pM, 50 pM, 100 pM, 200 pM, 500 pM, 1 nM, 2 nM, 5 nM, 10 nM, 20 nM, 50 nM, and 100 nM. b) cyclo-(γ-ImPyPyPyPy-(*R*)$^{H_2N}\gamma$-ImPyPyPyPy-) (**2**) lane 1: intact; lane 2: A reaction; lane 3: DNase I standard; lanes 4–19: 1 pM, 2 pM, 5 pM, 10 pM, 20 pM, 50 pM, 100 pM, 200 pM, 500 pM, 1 nM, 2 nM, 5 nM, 10 nM, 20 nM, 50 nM, and 100 nM. All reactions contain 30 kcpm restriction fragment, 10 mM Tris·HCl (pH 7.0), KCl (10 mM), $MgCl_2$ (10 mM) and $CaCl_2$ (5 mM). 5′-tAGAACTt-3′, 5′-tAGTACTt-3′, and 5′-tAGTACTt-3′ binding sites are shown on the right side of the autoradiograms.

Table 2. Relative polyamide specificities for 5′-tAGNNCTt-3′.[a,b]

	Polyamide	NN = 5′-AA-3′	5′-TA-3′	5′-AT-3′
1	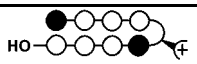	**2.5**	**5.3**	**1**
2	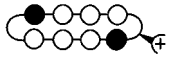	**8.0**	**14**	**1**
3	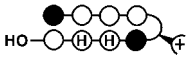	**4.4**	1.4	1
4	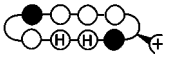	**75**	14	1
5	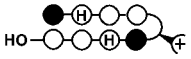	2.6	**70**	1
6	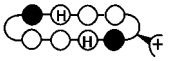	35	**320**	1
7	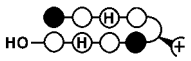	1	2.7	**1.4**
8	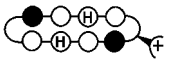	2.5	1	**4.4**

[a] The six base pair binding sites are annotated in capital letters such that NN = AA, TA, or AT. [b] Relative specificities of each compound for target sequences are calculated as K_a (respective site)/K_a (weakest site).

for this match site was enhanced with the cycle motif, cycle **2**, which exhibited 8- to 14-fold specificity for identical sites. This preference is consistent with previous reports[3e, 9] and may be due to the different microstructure of 5′-GA-3′ steps relative to 5′-GT-3′ steps. The contiguous Hp/Py pairings of cycle **4** affords a 16-fold enhanced binding to the 5′-tAGAACTt-3′ match site ($K_a = 7.5 \times 10^7\,M^{-1}$), relative to hairpin **3**, and five- to 75-fold specificity versus the other two single base pair mismatch sites. Cycle **6** with 5′-staggered Hp/Py pairs restores subnanomolar binding to the cognate 5′-tAGTACTt-3′ match site ($K_a = 3.2 \times 10^9\,M^{-1}$) with ten- and 320-fold specificity toward the single base pair mismatch site 5′-tAG**A**ACTt-3′ and double base pair mismatch 5′-tAG**AT**CTt-3′, respectively. It is surprising to note that a 3′-stagger of Hp/Py pairs in hairpin **7** selectively binds the double base pair mismatch 5′-tAG**TA**CT-3′ site with a twofold preference over the designed 5′-tAGATCTt-3′ match site. Perhaps preferential positioning of Hp/Py pairs within hairpin polyamides or DNA microstructure prevents favorable hairpin·DNA interactions at the match site. However, the cyclic analogue **8** reverses this mismatch preference, and effectively discriminates 5′-tAGATCT-3′ from 5′-tAG**TA**CT-3′ by enhancing affinity to the match sequence twofold, and providing fourfold specificity versus the double base pair mismatch site. These results illustrate that substitution of Py/Py with Hp/Py pairs in a cyclic

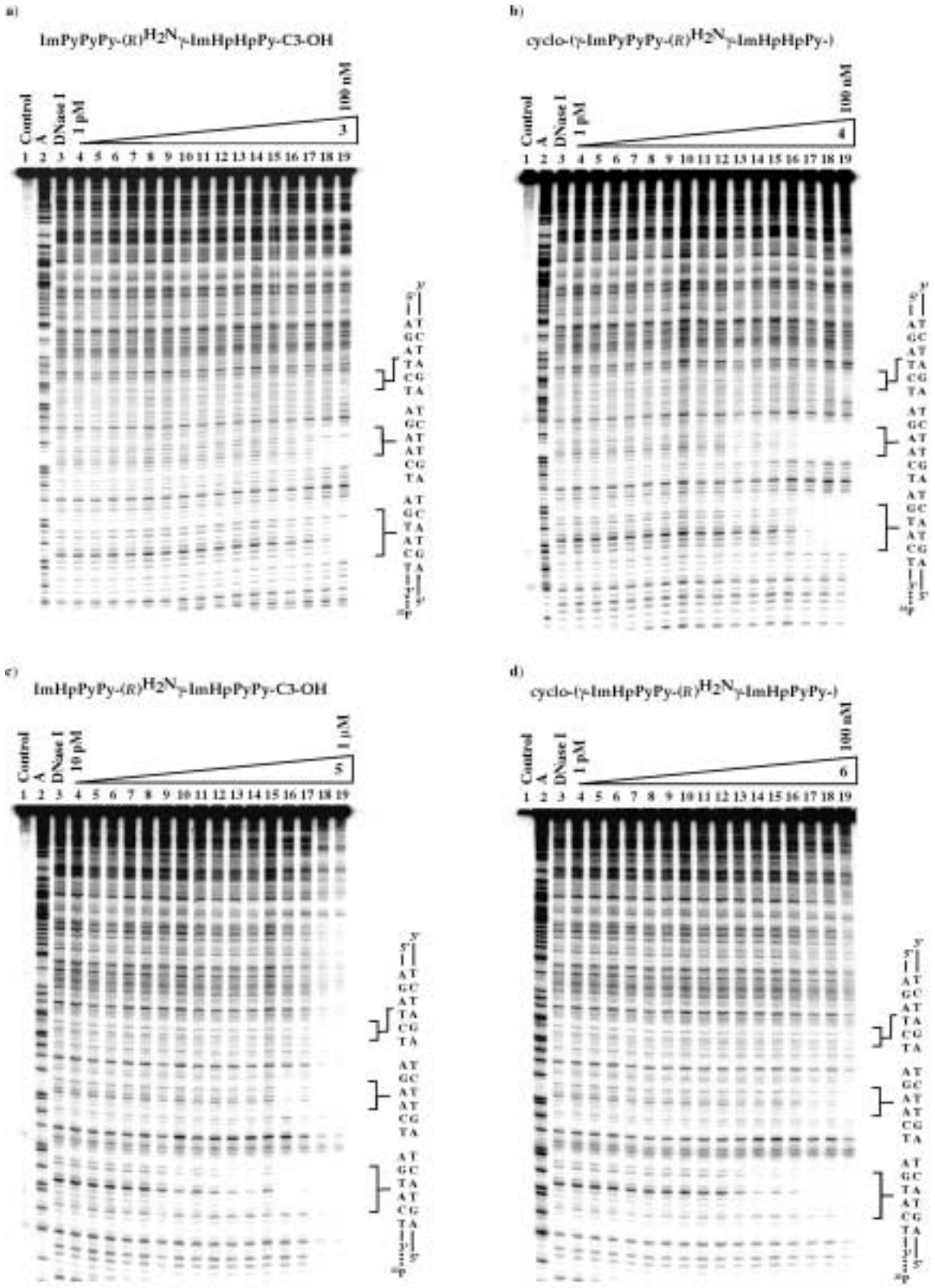

Figure 7. Footprinting experiments on the 3′-^{32}P-labeled 285-bp DNA restriction fragment derived from the plasmid pDEH10. Quantitative DNase I footprint titration experiment with a) ImPyPyPy-(*R*)$^{H_2N}\gamma$-ImHpHpPy-C3-OH (**3**): lane 1: intact; lane 2: A reaction; lane 3: DNase I standard; lanes 4–19: 1 pM, 2 pM, 5 pM, 10 pM, 20 pM, 50 pM, 100 pM, 200 pM, 500 pM, 1 nM, 2 nM, 5 nM, 10 nM, 20 nM, 50 nM, and 100 nM. b) cyclo-(γ-ImPyPyPy-(*R*)$^{H_2N}\gamma$-ImHpHpPy-) (**4**) lane 1: intact; lane 2: A reaction; lane 3: DNase I standard; lanes 4–19: 1 pM, 2 pM, 5 pM, 10 pM, 20 pM, 50 pM, 100 pM, 200 pM, 500 pM, 1 nM, 2 nM, 5 nM, 10 nM, 20 nM, 50 nM, and 100 nM. c) ImHpPyPy-(*R*)$^{H_2N}\gamma$-ImHpPyPy-C3-OH (**5**): lane 2: A reaction; lane 3: DNase I standard; lanes 4–19: 10 pM, 20 pM, 50 pM, 100 pM, 200 pM, 500 pM, 1 nM, 2 nM, 5 nM, 10 nM, 20 nM, 50 nM, 100 nM, 200 nM, 500 nM, and 1 μM. d) cyclo-(γ-ImHpPyPy-(*R*)$^{H_2N}\gamma$-ImHpPyPy-) (**6**) lane 1: intact; lane 2: A reaction; lane 3: DNase I standard; lanes 4–19: 1 pM, 2 pM, 5 pM, 10 pM, 20 pM, 50 pM, 100 pM, 200 pM, 500 pM, 1 nM, 2 nM, 5 nM, 10 nM, 20 nM, 50 nM, and 100 nM. All reactions contain 30 kcpm restriction fragment, Tris·HCl (10 mM, pH 7.0), KCl (10 mM), $MgCl_2$ (10 mM) and $CaCl_2$ (5 mM). 5′-tAGAACTt-3′, 5′-tAGTACTt-3′, and 5′-tAGATCTt-3′ binding sites are shown on the right side of the autoradiograms.

0947-6539/00/0624-4494 $ 17.50+.50/0 *Chem. Eur. J.* **2000**, *6*, No. 24

polyamide motif may be an effective strategy for discriminating multiple A•T/T•A base pairs with enhanced affinities but that 5′- versus 3′-stagger of Hp rings are quite different energetically.

Conclusion

It might have been expected that increasing the demand for optimal ligand–DNA interaction by introduction of multiple Hp pairs would have been detrimental to the binding affinity and specificity properties of the rigid cyclic polyamide motif in comparison to their respective hairpin counterparts. In contrast, we have demonstrated in this case that introduction of multiple Hp/Py pairs in a cyclic polyamide motif enhances DNA binding properties of 8-ring polyamides by increasing affinity relative to the hairpins while improving specificity toward 5′-tTGAACTt-3′ and 5′-tTGATCTt-3′ sites. Although these results indicate that employing a cyclic polyamide motif containing Hp/Py pairs to discriminate A/T sequences through minor groove recognition is viable, future studies will be required to test the general applicability of this approach and will be reported in due course.

Experimental Section

General: Dicyclohexylcarbodiimide (DCC), hydroxybenzotriazole (HOBt), 2-(1*H*-benzotriazole-1-yl)-1,1,3,3-tetramethyluronium hexafluorophosphate (HBTU), Boc-anhydride (Boc_2O), and 0.25 mmol g^{-1} Boc-β-alanine-(4-carboxamidomethyl)benzyl ester co-poly(styrene-divinylbenzene) resin (Boc-β-PAM-Resin) was purchased from Peptides International, USA. (*R*)-2-Fmoc-4-Boc-diaminobutyric acid and γ-aminobutyric acid (γ) were purchased from Bachem. *N*,*N*-Diisopropylethylamine (DIEA) and *N*,*N*-dimethylformamide (DMF) were purchased from Applied Biosystems. Dichloromethane (DCM) was reagent grade from EM; thiophenol (PhSH), dimethylaminopropylamine (Dp), diphenylphosphoryl azide (DPPA), piperidine, palladium acetate, potassium carbonate, and ammonium formate were from Aldrich. Trifluoroacetic acid (TFA) Biograde was from Halocarbon and *N*-(benzyloxycarbonyloxy) succimide (Cbz-OSu) was from Fluka. All reagents were used without further purification.

Quik-Sep polypropylene disposable filters were purchased from Isolab Inc. A shaker for manual solid-phase synthesis was obtained from St. John Associates, Inc. Screw-cap glass peptide synthesis reaction vessels (5 mL and 20 mL) with a No. 2 sintered glass frit were made as described by Kent.[10] UV spectra were measured in water on a Hewlett–Packard 8452A diode array spectrophotometer. Matrix-assisted, laser desorption/ionization time-of-flight mass spectrometry (MALDI-TOF) was performed at the Protein and Peptide Microanalytical Facility at the California Institute of Technology. HPLC analysis was performed on a Beckman Gold system using a RAINEN C_{18}, Microsorb MV, 5 μm, 300 × 4.6 mm reversed-phase column in 0.1% (*w*/*v*) TFA with acetonitrile as eluent and a flow rate of 1.0 mL min^{-1}, gradient elution 1.25% acetonitrile min^{-1}. Preparatory reversed-phase HPLC was performed on a Beckman HPLC with a Waters DeltaPak 25 × 100 mm, 100 μm C18 column equipped with a guard, 0.1% (*w*/*v*) TFA, 0.25% acetonitrile min^{-1}. Milli-Q water was obtained from a Millipore MilliQ water purification system, and all buffers were 0.2 μm filtered.

Polyamide synthesis: Reagents and protocols for polyamide synthesis were as previously described.[3c, 5, 7a] Polyamides were purified by reversed-phase HPLC on a Beckman HPLC with a Waters DeltaPak 25 × 100 mm, 100 μm C18 column equipped with a guard, 0.1% (*w*/*v*) TFA, 0.25% acetonitrile min^{-1}. Extinction coefficients were calculated based on $\varepsilon =$ 8333 per ring at 304 nm.[11]

General procedure for $NaBH_4$ cleavage:[8] The appropriate resin (100 mg) was placed in a sealable container and swollen in dry THF (1 mL). $NaBH_4$ (15 mg) was added subsequently, the vessel then sealed, and the reaction heated at 60 °C for 5 h. After cooling to room temperature, the reaction was quenched by addition of 20% TFA/80% H_2O (4 mL); CH_3CN (4 mL) was then added and the supernatant was collected by filtration. The resulting solution was frozen in liquid nitrogen, lyophilized, resuspended in 0.1% TFA/H_2O, and purified by reversed-phase HPLC to yield the appropriate polyamide.

ImPyPyPy-$(R)^{H_2N}\gamma$-ImOpOpPy-C3-OH (**9**): Recovered upon lyophilization of the appropriate fractions as a white powder (1 mg, 3%). MALDI-TOF-MS $[M+H]^+$ (monoisotopic): 1199.5; calcd for $C_{55}H_{67}N_{20}O_{12}$: 1199.5.

ImOpPyPy-$(R)^{H_2N}\gamma$-ImOpPyPy-C3-OH (**10**): Recovered upon lyophilization of the appropriate fractions as a white powder (0.9 mg, 3%). MALDI-TOF-MS $[M+H]^+$ (monoisotopic): 1199.5; calcd for $C_{55}H_{67}N_{20}O_{12}$: 1199.5.

ImPyOpPy-$(R)^{H_2N}\gamma$-ImPyOpPy-C3-OH (**11**): Recovered upon lyophilization of the appropriate fractions as a white powder (0.5 mg, 2%). MALDI-TOF-MS $[M+H]^+$ (monoisotopic): 1199.7; calcd for $C_{55}H_{67}N_{20}O_{12}$: 1199.5.

General procedure for $Pd(OAc)_2$/NH_4CO_2H cleavage:[7a] The appropriate resin (300 mg, 0.5 mmol g^{-1}, as synthesized in ref. [7a]) and $Pd(OAc)_2$ (300 mg) were placed in a sealable container, suspended in DMF (1 mL), and shaken at 37 °C for 3 h. NH_4CO_2H (700 mg), dissolved in H_2O (1 mL), was then added slowly over 3 min, the vessel sealed, and the resulting solution shaken at 37 °C for 12 hours. The supernatant was collected by filtration and subsequently purified by reversed-phase HPLC to yield the appropriate polyamide.

H_2N-γ-ImOpOpPy-$(R)^{Boc}\gamma$-ImPyPyPy-OH (**12**): Recovered upon lyophilization of the appropriate fractions as a white powder (7 mg, 4%). MALDI-TOF-MS $[M+H]^+$ (monoisotopic): 1342.7; calcd for $C_{61}H_{76}N_{21}O_{15}$: 1342.6.

H_2N-γ-ImOpPyPy-$(R)^{Boc}\gamma$-ImOpPyPy-OH (**13**): Recovered upon lyophilization of the appropriate fractions as a white powder (13 mg, 7%). MALDI-TOF-MS $[M+H]^+$ (monoisotopic): 1342.7; calcd for $C_{61}H_{76}N_{21}O_{15}$: 1342.6.

H_2N-γ-ImPyOpPy-$(R)^{Boc}\gamma$-ImPyOpPy-OH (**14**): Recovered upon lyophilization of the appropriate fractions as a white powder (5 mg, 3%). MALDI-TOF-MS $[M+H]^+$ (monoisotopic): 1342.7; calcd for $C_{61}H_{76}N_{21}O_{15}$: 1342.6.

General cyclization procedure:[7b] The appropriate precycle was dissolved in DMF (1 μmol per 5 mL), K_2CO_3 was added (10 mg per μmol polyamide) and the resulting solution stirred at RT for 30 min. DPPA (30 μL per μmol polyamide) was then added and the resulting solution stirred at room temperature for 5 h. The solution was filtered to remove excess K_2CO_3, and all volatiles in the filtrate were removed in vacuo. The resulting white powder was dissolved in TFA (2 mL) and allowed to stand at RT for 30 min. The volume was subsequently adjusted to 10 mL with 0.1% TFA/H_2O and purification by reversed-phase HPLC yielded the appropriate cyclic polyamide.

cyclo-(γ-ImPyPyPy-$(R)^{H_2N}\gamma$-I mOpOpPy-) (**15**): Recovered upon lyophilization of the appropriate fractions as a white powder (1.2 mg, 20%). MALDI-TOF-MS $[M+H]^+$ (monoisotopic): 1224.6; calcd for $C_{56}H_{66}N_{21}O_{12}$: 1224.5.

cyclo-(γ-ImOpPyPy-$(R)^{H_2N}\gamma$-ImOpPyPy-) (**16**): Recovered upon lyophilization of the appropriate fractions as a white powder (1.5 mg, 25%). MALDI-TOF-MS $[M+H]^+$ (monoisotopic): 1224.5; calcd for $C_{56}H_{66}N_{21}O_{12}$: 1224.5.

cyclo-(γ-ImPyOpPy-$(R)^{H_2N}\gamma$-ImPyOpPy-) (**17**): Recovered upon lyophilization of the appropriate fractions as a white powder (1.4 mg, 20%). MALDI-TOF-MS $[M+H]^+$ (monoisotopic): 1224.8; calcd for $C_{56}H_{66}N_{21}O_{12}$: 1224.5.

General O-demethylation procedure:[3e] NaH (100 mg), DMF (1 mL), thiophenol (0.5 mL) were heated at 100 °C for 10 min. The polyamide, dissolved in DMF (1 mL), was subsequently added and the resulting mixture heated at 100 °C for 2 h. After cooling to 22 °C, the solution was diluted to 10 mL with 20% TFA/80% H_2O, extracted with EtOAc (3×) and with Et_2O (2×), and the aqueous phase purified by reversed-phase HPLC to yield the appropriate polyamide.

ImPyPyPy-$(R)^{H_2N}\gamma$-ImHpHpPy-C3-OH (**3**): Recovered upon lyophilization of the appropriate fractions as a white powder (0.2 mg, 30%).

  0947-6539/00/0624-4495 $ 17.50+.50/0

MALDI-TOF-MS $[M+H]^+$ (monoisotopic): 1171.4; calcd for $C_{53}H_{63}N_{20}O_{12}$: 1171.5.

cyclo-(γ-ImPyPyPy-(*R*)^{H_2N}γ-ImHpHpPy-) (**4**): Recovered upon lyophilization of the appropriate fractions as a white powder (0.25 mg, 25%). MALDI-TOF-MS $[M+H]^+$ (monoisotopic): 1196.5; calcd for $C_{54}H_{62}N_{21}O_{12}$: 1196.5.

ImHpPyPy-(*R*)^{H_2N}γ-ImHpPyPy-C3-OH (**5**): Recovered upon lyophilization of the appropriate fractions as a white powder (0.18 mg, 30%). MALDI-TOF-MS $[M+H]^+$ (monoisotopic): 1171.5; calcd for $C_{53}H_{63}N_{20}O_{12}$: 1171.6.

cyclo-(γ-ImHpPyPy-(*R*)^{H_2N}γ-ImHpPyPy-) (**6**): Recovered upon lyophilization of the appropriate fractions as a white powder (0.2 mg, 35%). MALDI-TOF-MS $[M+H]^+$ (monoisotopic): 1196.5; calcd for $C_{54}H_{62}N_{21}O_{12}$: 1196.5.

ImPyOpPy-(*R*)^{H_2N}γ-ImPyOpPy-C3-OH (**7**): Recovered upon lyophilization of the appropriate fractions as a white powder (0.2 mg, 30%). MALDI-TOF-MS $[M+H]^+$ (monoisotopic): 1171.4; calcd for $C_{53}H_{63}N_{20}O_{12}$: 1171.5.

cyclo-(γ-ImPyHpPy-(*R*)^{H_2N}γ-ImPyHpPy-) (**8**): Recovered upon lyophilization of the appropriate fractions as a white powder (0.12 mg, 20%). MALDI-TOF-MS $[M+H]^+$ (monoisotopic): 1196.4; calcd for $C_{54}H_{62}N_{21}O_{12}$: 1196.5.

DNA reagents and materials: Enzymes were purchased from Boehringer Mannheim and used with their supplied buffers. Deoxyadenosine and thymidine 5′-[α-^{32}P] triphosphates were obtained from Amersham; deproteinized calf thymus DNA was acquired from Pharmacia. RNase free water was obtained from USB and used for all footprinting reactions. All other reagents and materials were used as received. All DNA manipulations were performed according to standard protocols.[12]

Construction of plasmid DNA: The plasmid pDEH10 was constructed by hybridization of oligos 5′-CTAGTGGATGCTGGTTAGTACTTG-GATGCTGGTAGAACTTGGATGCTGGTTAGATCTTG-GATGCTGGTTGCA-3′ and 5′-ACCAGCATCCAAGATCTAACCAG-CATCCAAGTTCTAACCAGCATCCAAGTACTAACCAGCATCCA-3′ followed by insertion into *Xba*I/*Pst*I linearized pUC19 plasmid using T4 DNA ligase. The resultant construct was used to transform Top10F′ OneShot competent cells from Invitrogen. Ampicillin-resistant white colonies were selected from 25 mL Luria–Bertani medium agar plates containing 50 μg mL^{-1} ampicillin and treated with XGAL and IPTG solutions. Large-scale plasmid purification was performed with Qiagen Maxi purification kits. Dideoxy sequencing was used to verify the presence of the desired insert. Concentration of the prepared plasmid was determined at 260 nm using the relationship of 1 OD unit = 50 μg mL^{-1} duplex DNA.

Preparation of 3′-end-labeled restriction fragments: The plasmid pDEH10 was linearized with *Eco*RI and *Pvu*II, then treated with the sequenase enzyme, deoxyadenosine 5′-[α-^{32}P]triphosphate and thymidine 5′-[α-^{32}P]triphosphate for 3′ labeling. The labeled 3′ fragment was loaded onto a 6% nondenaturing polyacrylamide gel, and the desired 285 base-pair band was visualized by autoradiography and isolated. Chemical sequencing reactions were performed according to published methods.[13]

DNase I footprinting:[6] All reactions were carried out in a volume of 400 μL. We note explicitly that no carrier DNA was used in these reactions until after DNase I cleavage. A polyamide stock solution or water (for reference lanes) was added to an assay buffer where the final concentrations were: Tris·HCl buffer (10 mM, pH 7.0), KCl (10 mM), $MgCl_2$ (10 mM), $CaCl_2$ (5 mM), and 30 kcpm 3′-radiolabeled DNA. The solutions were allowed to equilibrate for 4 h at 22 °C. Cleavage was initiated by the addition of 10 μL of a DNase I stock solution (diluted with 1 mM DTT to give a stock concentration of 1.875 u per mL) and was allowed to proceed for 7 min at 22 °C. The reactions were stopped by adding 50 μL of a solution containing NaCl (2.25 M), EDTA (150 mM), glycogen (0.6 mg mL^{-1}), and base-pair calf thymus DNA (30 μM), and then precipitated with ethanol. The cleavage products were resuspended in 100 mM tris-borate-EDTA/80% formamide loading buffer, denatured at 85 °C for 6 min, and immediately loaded onto an 8% denaturing polyacrylamide gel (5% crosslink, 7 M urea) at 2000 V for 1 h. The gels were dried under vacuum at 80 °C, then quantitated using storage phosphor technology.

Equilibrium association constants were determined as previously described.[6a] The data were analyzed by performing volume integrations of the 5′-AGAACT-3′, 5′-AGTACT-3′, and 5′-AGATCT-5′ sites and a reference site. The apparent DNA target site saturation, θ_{app}, was calculated for each concentration of polyamide using Equation (1):

$$\theta_{app} = 1 - \frac{I_{tot}/I_{ref}}{I^0_{tot}/I^0_{ref}} \quad (1)$$

where I_{tot} and I_{ref} are the integrated volumes of the target and reference sites, respectively, and I^0_{tot} and I^0_{ref} correspond to those values for a DNase I control lane to which no polyamide has been added. The ($[L]_{tot}$, θ_{app}) data points were fit to a Langmuir binding isotherm [Eq. (2), $n = 1$ for polyamides **1**–**8**] by minimizing the difference between θ_{app} and θ_{fit}, using the modified Hill equation:

$$\theta_{fit} = \theta_{min} + (\theta_{max} - \theta_{min}) \frac{K_a^n [L]_{tot}^n}{1 + K_a^n [L]_{tot}^n} \quad (2)$$

where $[L]_{tot}$ corresponds to the total polyamide concentration, K_a corresponds to the equilibrium association constant, and θ_{min} and θ_{max} represent the experimentally determined site saturation values when the site is unoccupied or saturated, respectively. Data were fit using a nonlinear least-squares fitting procedure of KaleidaGraph software (Version 2.1, Abelbeck software) with K_a, θ_{max}, and θ_{min} as the adjustable parameters. At least three sets of acceptable data were used in determining each association constant. All lanes from each gel were used unless visual inspection revealed a data point to be obviously flawed relative to neighboring points. The data were normalized using Equation (3):

$$\theta_{norm} = \frac{\theta_{app} - \theta_{min}}{\theta_{max} - \theta_{min}} \quad (3)$$

Quantitation by storage phosphor technology autoradiography: Photostimulable storage phosphorimaging plates (Kodak Storage Phosphor Screen S0230 obtained from Molecular Dynamics) were pressed flat against gel samples and exposed in the dark at 22 °C for 12–20 h. A Molecular Dynamics 400S PhosphorImager was used to obtain all data from the storage screens. The data were analyzed by performing volume integrations of all bands using the ImageQuant v. 3.2.

Acknowledgement

We are grateful to the National Institutes of Health (GM-27681) for research support, the Treadway Foundation (Bio.47123-1-EN-DOW.471230) for a research award to D.M.H., and the National Institutes of Health (GM19789-02) for a postdoctoral fellowship to C.M. We thank G. M. Hathaway for MALDI-TOF mass spectrometry and S. White for construction of pDEH10.

[1] a) J. M. Gottesfeld, L. Nealy, J. W. Trauger, E. E. Baird, P. B. Dervan, *Nature* **1997**, *387*, 202–205; b) L. A. Dickinson, R. J. Gulizia, J. W. Trauger, E. E. Baird, D. E. Mosier, J. M. Gottesfeld, P. B. Dervan *Proc. Natl. Acad. Sci. USA* **1998**, *95*, 12890–12895.

[2] P. B. Dervan, R. W. Burli, *Curr. Opin. Chem. Biol.* **1999**, 3, 688–693.

[3] a) S. White, J. W. Szewczyk, J. M. Turner, E. E. Baird, P. B. Dervan, *Nature* **1998**, *391*, 468–471; b) C. L. Kielkopf, S. White, J. W. Szewczyk, J. M. Turner, E. E. Baird, P. B. Dervan, D. C. Rees, *Science* **1998**, *282*, 111–115; c) A. R. Urbach, J. W. Szewczyk, S. White, J. M. Turner, E. E. Baird, P. B. Dervan, *J. Am. Chem. Soc.* **1999**, *121*, 11621–11629; d) S. White, J. M. Turner, J. W. Szewczyk, E. E. Baird, P. B. Dervan, *J. Am. Chem. Soc.* **1999**, *121*, 260–261; e) C. L. Kielkopf, R. E., Bremer, S. White, J. W. Szewczyk, J. M. Turner, E. E. Baird, P. B. Dervan, D. C. Rees, *J. Mol. Biol.* **2000**, *295*, 557–567.

[4] J. W. Trauger, E. E. Baird, M. Mrksich, P. B. Dervan, *J. Am Chem. Soc.* **1996**, *118*, 6160–6166.

[5] E. E. Baird, P. B. Dervan, *J. Am. Chem. Soc.* **1996**, *118*, 6141–6146.

[6] a) M. Brenowitz, D. F. Senear, M. A. Shea, G. K. Ackers, *Methods Enzymol.* **1986**, *130*, 132–181; b) M. Brenowitz, D. F. Senear, M. A. Shea, G. K. Ackers, *Proc. Natl. Acad. Sci. USA* **1986**, *83*, 8462–8466;

  0947-6539/00/0624-4496 $ 17.50+.50/0

c) D. F. Senear, M. Brenowitz, M. A. Shea, G. K. Ackers, *Biochemistry* **1986**, *25*, 7344–7354.
[7] a) D. M. Herman, E. E. Baird, P. B. Dervan, *J. Am. Chem. Soc.* **1999**, *121*, 1121–1129; b) J. Cho, M. E. Parks, P. B. Dervan, *Proc. Natl. Acad. Sci. USA* **1995**, *92*, 10389–10392.
[8] a) A. R. Mitchell, S. B. Kent, M. Engelhard, R. B. J. Merrifield, *J. Org. Chem.* **1978**, *43*, 2845–2852; b) J. M. Stewart, J. D. Young, *Solid Phase Peptide Synthesis*, Pierce Chemical Company, Rockfor IL, **1984**.
[9] S. White, E. E. Baird, P. B. Dervan, *Biochemistry* **1996**, *35*, 12532–12537.
[10] S. B. H. Kent, *Annu. Rev. Biochem.* **1988**, *57*, 957–989.
[11] D. S. Pilch, N. A. Pokar, C. A. Gelfand, S. M. Law, K. J. Breslauer, E. E. Baird, P. B. Dervan, *Proc. Natl. Acad. Sci. USA* **1996**, *93*, 8306–8311.
[12] J. Sambrook, E. F. Fritsch, T. Maniatis, *Molecular Cloning*, Cold Spring Harbor Laboratory, Cold Spring Harbor, NY, **1989**.
[13] a) B. L. Iverson, P. B. Dervan, *Nucl. Acids Res.* **1987**, *15*, 7823–7830; b) A. M. Maxam, W. S. Gilbert, *Methods Enzymol.* **1980**, *65*, 499–560.
[14] W. S. Wade, M. Mrksich, P. B. Dervan, *J. Am. Chem. Soc.* **1992**, *114*, 8783–8794.

Received: August 11, 2000 [F2672]

  0947-6539/00/0624-4497 $ 17.50+.50/0